Effects of feed solution pretreatment on pressure-retarded osmosis: changes in dissolved organic matter according to fluorescence excitation-emission matrix spectroscopy coupled with parallel factor analysis and liquid chromatography-organic carbon detection

Sookhyun Nam[a], Jae-Wuk Koo[a], Eunju Kim[a], Seong-Nam Nam[b], Tae-Mun Hwang[a,*]

[a]Korea Institute of Civil Engineering and Building Technology, Dae-hwa-Dong 283, Goyangdae-Ro, Ilsanseo-Gu, Goyang-Si, Gyeonggi-Do, 10223, Republic of Korea, Tel. +82-31-910-0741; Fax: +82-31-910-0291; emails: taemun@kict.re.kr (T.-M. Hwang), fpnsh@kict.re.kr (S. Nam), koojaewuk@kict.re.kr (J.-W. Koo), kej@kict.re.kr (E. Kim)
[b]Department of Civil and Environmental Engineering, Chung-Ang University, 84 Heukseok-ro, Dongjak-gu, Seoul, Republic of Korea, email: namsn76@gmail.com

ABSTRACT

Pressure-retarded osmosis (PRO) is the next generation seawater desalination technology, and is considered an eco-friendly and economic renewable energy. As such, there have been studies on methods of efficient cleaning to restore degraded membrane performance due to the reversible membrane fouling that inevitably occurs after prolonged operation. Owing to the fact that fouling occurs differently in each type of pretreatment process involved in PRO, it is important to understand the type of organic matter that causes fouling in each of the PRO pretreatment processes. In this study, the composition of dissolved organic matter (DOM) was characterized and assessed among membrane bioreactor, ultrafiltration, activated carbon/sand filter, and low-pressure reverse osmosis PRO pretreatment processes. The characteristics of DOM that caused fouling in the PRO membrane was identified using fluorescence excitation-emission matrix spectroscopy (F-EEMs) coupled with parallel factor analysis (PARAFAC) and a liquid chromatography-organic carbon detector (LC-OCD) technique. The major components could be summarized as microbial humic-like fluorescence, humic and fulvic substances, terrestrial humic-like fluorescence in high nutrient and wastewater-influenced environments, and tryptophan-like substances. The foulants that affected the PRO membrane were found to be humic and fulvic substances as a result of the PARAFAC analysis and humic substances and building blocks as a result of the LC-OCD analysis.

Keywords: Foulant; Pressure-retarded osmosis; Pretreatment; Fluorescence excitation-emission matrix spectroscopy; Parallel factor analysis

1. Introduction

Seawater desalination is a method of securing a stable supply of water resources that is unaffected by climate change. It has been widely applied in the Middle Eastern region; however, markets have recently expanded into North America, Australia, South America, Southeast Asia, China, and Europe.

The importance of conserving energy use in the desalination process has been highlighted in recent years [1]. Reverse osmosis (RO) is a rapidly growing desalination method as it can obtain fresh water with relatively low energy compared with the existing distillation method. Current RO technology has been developed to its maximum level, so ways of combining pressure-retarded osmosis (PRO) with RO are being studied to lower the operating energy. PRO involves technologies

* Corresponding author.

that use the osmotic energy differences between two solutions with substantial salinity differences (i.e., high and low salinity) to produce energy [2,3]. This is an osmotically driven membrane process where water flows from a low osmotic pressure feed solution (FS) to a high osmotic pressure draw solution (DS) against hydraulic pressure [4]. In practice, various water sources, such as river water, impaired water or pretreated wastewater effluent, and brackish water, can be used as FS in the PRO process. In particular, organic foulants in the FS that are smaller than the membrane pores exist in any kind of water source, which can cause serious internal membrane fouling when using a PRO membrane [5]. Therefore, it is necessary to introduce a pretreatment method that prevents foulants from developing during the application of FS, such as pretreated wastewater effluent, when designing PRO. According to previous studies, various methods, such as low-pressure reverse osmosis (LPRO), ultrafiltration (UF), ultraviolet (UV), and ozone treatments, have been used, and three-dimensional excitation-emission matrix fluorescence spectroscopy has been applied to evaluate potential foulants [6–8]. The major substance that causes fouling in the PRO membrane is dissolved organic matter (DOM). DOM is often used as a design parameter owing to its removal efficiency and characteristics in the design of water treatment processes. Understanding the major foulants in the PRO pretreatment process is an approach that can improve overall water quality and reduce membrane contamination. Understanding the major foulants associated with the membrane process plays an important role in choosing the filtration and cleaning strategy. Recently, cases of applying fluorescence excitation-emission matrix spectroscopy (F-EEMs) to the analysis of DOM have increased [9,10], and F-EEMs has been successfully utilized to obtain structural information on relatively low organic matter [11]. F-EEMs is represented as the emission and excitation wavelength function, and recently, F-EEMs of organic matter have been incorporated with multivariate data analyses [12]. Parallel factor analysis (PARAFAC) is commonly used, which can decompose F-EEMs of a sample into several independent fluorescent materials [13,14]. These techniques help to analyze major membrane foulants, such as extracellular polymeric substances and soluble microbial products that are hydrophilic and have high molecular weight [15]. F-EEMs coupled with PARAFAC have been used in a variety of applications, including water quality, pollution, and DOM monitoring, which cause membrane fouling [16–18]. Overall, F-EEMs-PARAFAC helps to evaluate the composition, distribution, and dynamics of DOM in aquatic environments [19]. Another advanced technique used to characterize DOM is liquid chromatography-organic carbon detection (LC-OCD) [20,21]. Combining LC-OCD with F-EEMs provides additional information on DOM characteristics. In this study, four pretreatment processes were tested to utilize pretreated wastewater effluent as FS in PRO. The pretreatment processes included membrane bioreactor (MBR), ultrafiltration (UF), low-pressure reverse osmosis (LPRO), and activated carbon/sand filter (AC/S) treatments. The flux reduction in the PRO process was compared according to the FS from each pretreatment process. Then, the characteristics of DOM contained in the pretreated water were analyzed using F-EEMs-PARAFAC and LC-OCD to observe the organic matter that caused the most fouling in the PRO membrane. In addition,

through the F-EEMs-PARAFAC analysis, the correlation between the fluorescence intensity of the PRO pretreated water and the UV absorbance at 254 nm (UV254) and DOC of the samples was investigated using the component score [22]. This investigation will help to understand the DOM characteristics of FS that affect the PRO membrane and to evaluate the performance of the PRO pretreatment processes through simple spectroscopic monitoring. This will enable the quantitative and qualitative evaluation of organic matter in the PRO pretreated water, and ultimately the creation of a continuous PRO pretreatment process monitoring system.

2. Materials and methods

2.1. Laboratory-scale pressure-retarded osmosis test device

A cross-flow experimental setup was used in this study, as shown in Fig. 1. The operating method for the PRO was active layer toward DS. The PRO membrane cell for the flat-sheet membrane was made of steel use stainless and had an effective membrane area of 0.0064 m^2 (0.08 m length × 0.08 m width). The applied pressure in the DS and pressure resistance in the FS were monitored using an electronic pressure gauge (GR200 Graphic Recorder, Hanyoung Nux, Korea). To measure water flux and power density, an electronic scale (Ranger 7000, Ohaus, USA) was placed under the FS container and the decrease in the amount of water was recorded. The operational mode consisted of having the PRO membrane arranged so that its active layer faced the DS and the DS and FS flow within the membrane cell formed a counter current. The water flux was calculated based on the changes in the weight of the water. A thermostatic bath (RW-0525G, Jeiotech, Korea) was used to maintain a stable temperature (at 20°C for both the DS and FS). Pressure conditions were controlled using a booster pump (Hyosung, Korea). The DS was made from NaCl (SAMCHUN, Korea) with a concentration of 1.2 M. In theory, the maximum power density could be achieved at 25–30 bar when applying PRO operations using a NaCl solution with a concentration of 1.2 M. The operational pressure of the DS was set at 15 bar. In order to make use of a DS similar to the RO brine concentration, a 1.2 M NaCl solution was used. Flow rates of both the FS and DS were fixed at 1 LPM, and the volumes of the FS and DS were maintained at 2 L.

2.2. Pretreated water for pressure-retarded osmosis

The FS of the PRO process was water that was pretreated using four processes. The treatment processes consisted of UF, MBR, AC/S, and LPRO. UF, AC/S and LPRO were effluent pre-treated water. The membrane used for the UF and MBR processes was a hollow fiber type made of polyvinylidene difluoride with a pore size of 0.1 μm (MR-MHP07A, LG Corporation, Korea), and for the LPRO pretreatment, a RO membrane (RE2540-BN, Toray Chemical, Korea) was used. The AC/S was a filter paper composed of activated carbon and sand.

2.3. Analytical methods

All samples were filtered using a 0.45 μm cellulose acetate membrane filter prior to analysis. The DOC of the
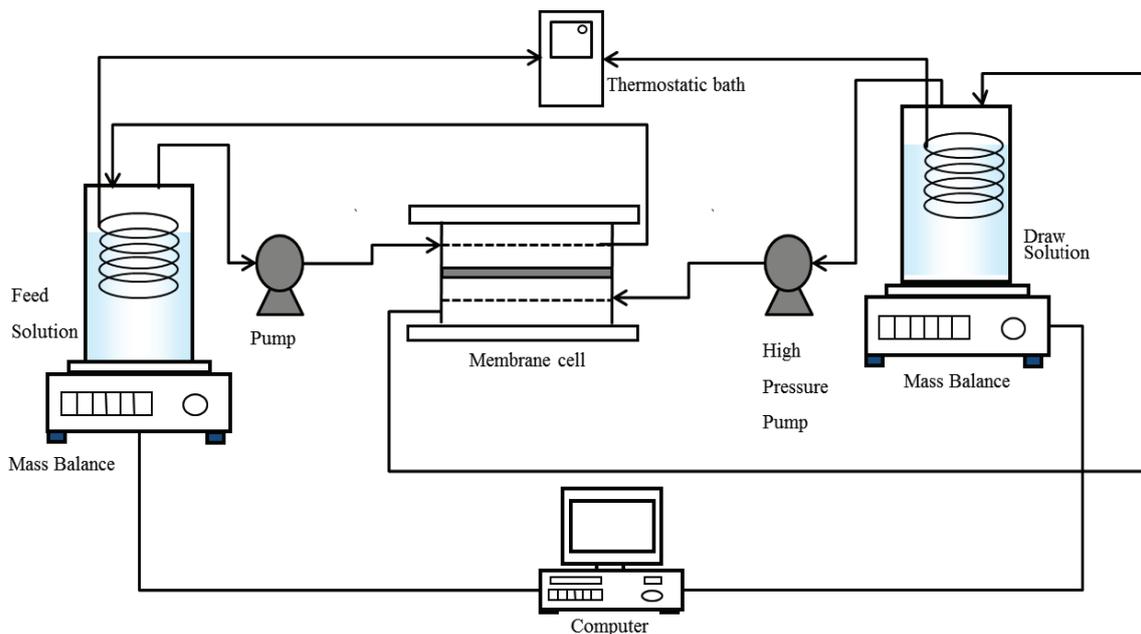
Fig. 1. Schematic of the laboratory-scale pressure-retarded osmosis system.

sample was measured using a total organic carbon (TOC) analyzer (Shimadzu TOC-V$_{\text{CPH}}$, Japan), and UV254 was measured using a UV/V is spectrophotometer (DR 5000, HACH, USA). Total nitrogen (TN) and total phosphorus (TP) were analyzed using a multi-parameter water quality analyzer (SYNCA 3CH, Germany). The F-EEMs of samples were obtained using an Aqualog fluorometer (Horiba, Japan) by scanning excitation wavelengths of 250–550 nm at 2 nm intervals and emission wavelengths of 250–800 nm at 2.33 nm intervals. The scanning speed and integration time were 500 nm/s and 0.5 s, respectively. Corrected F-EEMs were obtained in accordance with published methods [23–25]. F-EEMs of ultrapure water were subtracted from the F-EEMs of the samples, followed by normalizing the F-EEMs with the area of the water Raman peak measured on the same day as the samples. For the molecular weight (MW) distribution of DOM, the LC-OCD system manufactured by DOC-LABOR (Karlsruhe, Germany) was used. The system consisted of an auto-injector, size exclusion column (TSK-HW-50S, 250 mm × 20 mm, Tosoh, Japan), and thin film reactor, which oxidized the components divided from the column into CO_2, and a UV254 detector and non-dispersive infrared detector.

2.4. Parallel factor analysis modeling

PARAFAC is one of the multi-way decomposition methods that is widely used for quantitative understanding of DOM. Under ideal conditions where F-EEMs independently follow Beer's Law, each EEM presents fluorescence from the underlying fluorescence; based on this principle, the method of analyzing EEM by presenting them three-dimensionally is referred to as 3D-PARAFAC modeling. The general principle of 3D-PARAFAC modeling involves the division of EEM data into three modes, namely *a*, *b*, and *c*, to undertake a three-dimensional analysis. The following equation represents 3D-PARAFAC modeling [26,27].

$$X_{ijk} = \sum_{f=1}^{F} a_{if} b_{if} c_{kf} + \varepsilon_{ijk}, \qquad (1)$$
$$i = 1, 2 \ldots I; \ j = 1, 2 \ldots J; \ k = 1, 2 \ldots K;$$

where x_{ijk} is one element of the three-way data array with dimensions *i*, *j*, and *k*.

x_{ijk} refers to the emission wavelength *j*, excitation wavelength *k*, and fluorescence intensity measured from sample *i*. The created model is based on parameters *a*, *b*, and *c*. This represents the concentration, emission spectra, and excitation spectra for each component, respectively. The component scores represent the relative density of the representative organic matter of the components. *F* refers to the number of components. Excitation and emission loadings present the characteristics of the excitation and emission spectra [19,28]. The F-EEMs data were analyzed using the PARAFAC algorithm within the Eigenvector, Inc. Solo Package (Aqualog, Horiba, Japan). PARAFAC analysis was conducted through modeling based on 70 EEM fluorescence data. The number of fluorescence components was determined by validating with analysis of variance (ANOVA), core consistency diagnostic and split-half analysis. The maximum fluorescence intensities ($F_{\max}$) of each substance represent the relative intensities of the substance concerned in the sample, and the excitation and emission loading values present the characteristics of the excitation and emission spectra.

3. Results and discussion

3.1. Power density and flux decline

PRO processes use the osmotic energy differences between two solutions (high-density saline solution and low-density saline solution) to produce energy. The PRO technology examined in this study was related to a technology that combines the use of wastewater and seawater. That is,

wastewater effluents or process water of wastewater treatment facilities were used as the FS of the PRO process, and a RO concentrate of a seawater desalination system were used as the DS. The power that could be produced per unit membrane area (i.e., power density) in the PRO process was equal to the product of the water flux and the hydraulic pressure differential across the membrane [29].

$$W = J_w \Delta P = A(\Delta\pi - \Delta P)\Delta P \tag{2}$$

where W is the power density (W/m^2), J_w is the water flux (L (m^2·h)$^{-1}$), A is the water permeability coefficient, $\Delta\pi$ is the osmotic pressure differential, and ΔP is the hydraulic pressure differential. This equation describes the diffusive transport of water through the PRO membrane. The power density is proportional to the hydraulic pressure differential and water flux across the membrane. As shown in Eq. (2), the osmotic pressure is converted to mechanical energy. In ideal conditions, the hydraulic pressure increases as the water flux decreases unless ΔP reaches zero ($\Delta P = \Delta\pi$, namely the flux reversal point). The maximum power density is achieved when ΔP is equal to $\Delta\pi/2$, and then decreases with flux reversal.

$$W_{max} = A\frac{\Delta\pi^2}{4} \tag{3}$$

This study examined the influence of the organic matter content in water on PRO power densities. UF-treated water, LPRO-treated water, and LPRO concentrate were mixed to control the organic matter concentration. The FS was prepared to have TOC content within the range of 1~10 mg L^{-1}. Fig. 2 shows the positive dependency of the maximum power density on the TOC content of the FS. As indicated in Fig. 2, a high correlation ($R^2 = 0.97$, $p < 0.05$) was found between the PRO power densities and TOC, thereby indicating that organic matter was one of the major parameters affecting PRO performance.

Four types of water with a different extent of pretreatment were used as FS of the experiments. First, effluents taken from the Ilsan sewage treatment plant (Goyang-si, South Korea) were pretreated by UF, MBR, AC/S, and LPRO. Table 1 summarizes the characteristics of the water used as the PRO FS, and the flux declines were compared depending on the FS (Fig. 3). Fig. 3 shows the flux decline of the pretreated water used as FS in the PRO process.

Fig. 2. Correlation between power density and the total organic carbon (TOC) content at 15 bar draw solution.
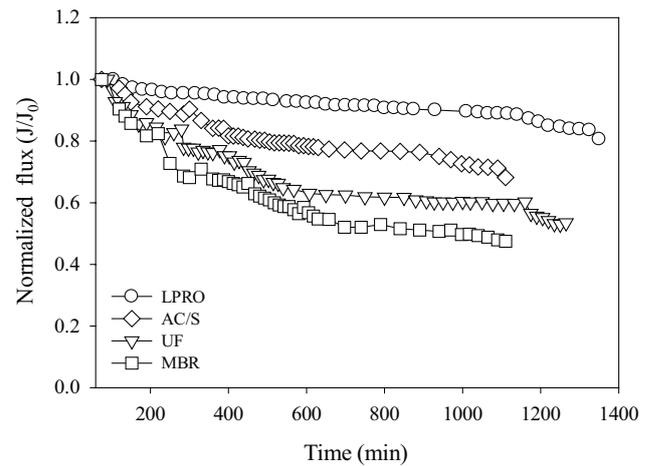
Fig. 3. Changes in the normalized flux over time depending on the pressure-retarded osmosis pretreatments.

Table 1
Quality of the sewage effluent (i.e., before pretreatment) and pretreated water

Parameters	Feed water	Pre-treated water			
		UF	AC/S	MBR	LPRO
Total coliform (No./mL)	2,280 ± 10	0 ± 1	0 ± 1	0 ± 1	0 ± 0
Turbidity (NTU)	8.06 ± 2.00	0.065 ± 0.004	0.090 ± 0.005	0.090 ± 0.005	0.040 ± 0.001
UV254 (cm^{-1})	0.115 ± 0.002	0.109 ± 0.001	0.011 ± 0.002	0.111 ± 0.002	0.004 ± 0.001
TDS (mg L^{-1})	524 ± 5	523 ± 5	520 ± 5	520 ± 5	80 ± 5
pH	6.88 ± 0.2	6.89 ± 0.2	6.89 ± 0.2	6.89 ± 0.2	6.87 ± 0.2
TOC (mg L^{-1})	7.63 ± 0.3	6.73 ± 0.3	0.78 ± 0.3	7.23 ± 0.3	0.40 ± 0.1
DOC (mg L^{-1})	7.36 ± 0.3	6.62 ± 0.3	0.72 ± 0.3	6.88 ± 0.3	0.40 ± 0.1
Color (pt)	29 ± 2	27 ± 2	10 ± 2	28 ± 2	1 ± 0
T-N (mg L^{-1})	9.94 ± 0.1	9.03 ± 0.1	2.03 ± 0.1	8.03 ± 0.1	1.03 ± 0.2
T-P (mg L^{-1})	0.37 ± 0.05	0.34 ± 0.05	0.30 ± 0.05	0.24 ± 0.05	0.05 ± 0.1

As shown in Table 1, the turbidities of the pretreated water were not significantly different. However, the DOC and UV254 of the UF or MBR-treated water were much higher than those of the AC/S or LPRO-treated water. In the case of TN and TP, TN was slightly removed from the UF or MBR-treated water. About 79% of TN was removed from the AC/S-treated water, and about 89% of TN was removed from the LPRO-treated water. TP was removed in the order of LPRO, MBR, AC/S, and UF-treated water. These results showed that the concentration of organic matter was higher in the UF and MBR-treated water. It took approximately 10 h for the J/J_0 value of the UF-treated water to decrease to 0.6 and more than 20 h for the J/J_0 value of the AC/S-treated

water to decrease to 0.6. The UF-treated water showed a membrane contamination rate that was 3 times faster than that of the AC/S-treated water. These results showed that the organic matter in the FS was closely related to the power density and rate of flux decline.

3.2. Fluorescence excitation-emission matrix analysis of pretreated water

Fig. 4 presents the F-EEMs contour plots of the UF, AC/S, MBR, and LPRO-treated water. The main foulants of the UF process showed various functional groups, which had various molecular sizes and were composed of a complex

(a)

(b)

(c)

(d)

(e)
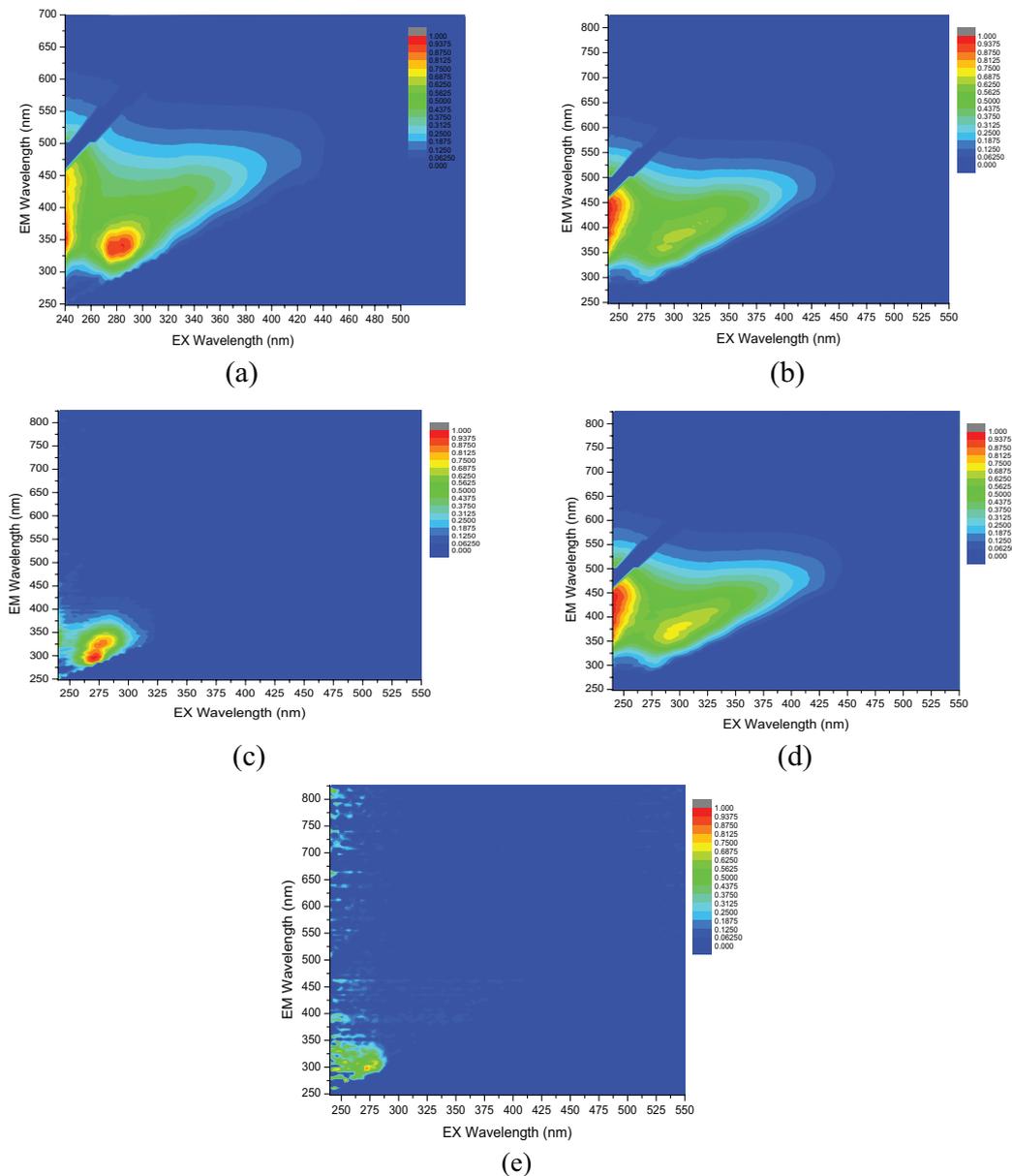
Fig. 4. 3D excitation-emission matrix (EEM) fluorescence spectra of (a) sewage effluent (S.E) without pretreatment, (b) ultrafiltration (UF)-treated, (c) activated carbon/sand filter (AC/S)-treated, (d) membrane bioreactor (MBR)-treated and (e) low-pressure reverse osmosis (LPRO)-treated effluent. The dissolved organic carbon concentrations of the samples were 6.2, 5.4, 0.7, 5.0, and 0.3 mg/L, respectively.

mixture of humic acids, fulvic acids, and proteins. Detailed informations measured by F-EEMs are summarized in Table 2, which is compared with the previously published paper [30]. The F-EEMs of sewage wastewater effluent before pretreatment showed intense peaks over regions I through IV (Table 2), with the maxima at regions I (tryptophan-like fluorophores; λ_{ex} = 270~280 nm and λ_{em} = 320~350 nm) and II (tryptophan-like fluorophores; λ_{ex} = 270~280 nm and λ_{em} = 320~350 nm). After the UF or MBR treatments, it was revealed that a tryptophan-like peak (Region II) and tyrosine-like peak (Region I) were removed rather than the humic-like fluorophores at Region III, thereby resulting in a shifting of the maximum Ex/Em position to < 250 nm/420~450 nm (Region III). Meanwhile, the F-EEMs after the AC/S or LPRO treatment displayed a significant disappearance of most of the peaks, and low or trace-level peaks in the protein-like region (Region II) remained.

The flow rates of the feed solution (FS) and draw solution (DS) were 1 LPM, and ultrafiltration (UF), membrane bioreactor (MBR), activated carbon/sand filter (AC/S), and low-pressure reverse osmosis (LPRO)-treated water were used for the FS. The DS was 1.2 M NaCl. The pressure of the DS was maintained at 25 bar. Flux data were obtained once per minute, and the mean value for 20 min was used.

3.3. Parallel factor analysis components

Seventy F-EEMs for pretreated PRO samples were analyzed, and three components were identified through PARAFAC analysis. Outliers were removed for the purpose of not only validating the model using the split-half method, but also facilitating the modeling process. The three-component model accounted for 97.3% of the entire variance. The split-half validation match was 98.6% and the core consistency was 94%. Fig. 5 presents the excitation and emission wavelengths of the main peaks. Table 3 presents the maxima of the excitation and emission wavelengths of the three components, and also presents explanations of similar components reported in other studies. The comparison of the components of this study to those of other studies indicated that the pretreated water for FS of PRO included both humic-like and protein-like fluorophores. Based on the spectral positions/shapes, it was thought that C1 and C2 were humic-like fluorophores that occur terrestrially or anthropogenically, while C3 were tryptophan-like (protein-like) fluorophores. The developed model was split-half validated. To determine

the quantitative changes in each component of the pretreated water, the fractions of the components were calculated from the PARAFAC results.

3.4. Parallel factor analysis component changes according to each process

Fig. 6 presents the F_{max} values of the UF, AC/S, MBR, and LPRO-treated water. The F_{max} values after each pretreatment represent the relative intensities of each component in the PARAFAC model. The PARAFAC results showed that of the components in the sewage effluent (before pretreatment),
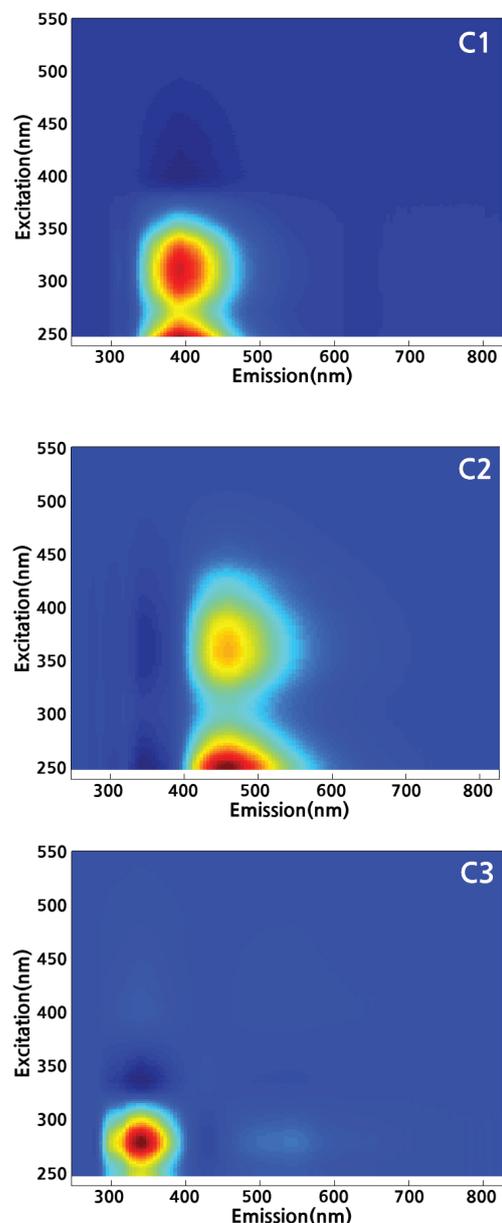
Fig. 5. Contour plots of the three components identified from the parallel factor analysis model; (a) component 1, (b) component 2, and (c) component 3.

Table 2
Fluorescence regions and excitation-emission wavelength boundaries (previously identified by Leenheer et al.) [30]

Region	$\lambda_{ex}/\lambda_{em}$ range (nm)	Description
I	270~280/300~320	Aromatic proteins and tyrosine-like substances
II	270~280/320~350	Aromatic proteins and tryptophan-like substances
III	250~260/380~480	Fulvic-like and humic-like substances
IV	330~350/420~480	Humic-like substances

C1 (F_{max} = 14.57) was the most abundant, followed by C2 and C3 (F_{max} values of 11.56 and 6.95, respectively), which corresponded to 44%, 35%, and 21% of the identified fluorophores, respectively. In addition, as expected from the previous results shown in Fig. 4, the UF or MBR processes did not effectively treat the three components (i.e., fluorophores) as the F_{max} values of the UF or MBR-treated water were almost the same as those of the sewage effluent. However, the AC/S or LPRO pretreatments removed the majority of C1 and C2, while a substantial portion of C3, which accounted for 84% (AC/S) and 71% (LPRO) of residual DOC, remained after the treatments. For better understanding of the pretreatments of organic matter in terms of MW, which could not be directly obtained by the PARAFAC analysis [35,40], the samples were further measured using LC-OCD.

3.5. Liquid chromatography with organic carbon detection (LC-OCD)

The DOM of pretreated samples was separated into each constituent by its MW. In the MW distribution of the chromatogram as shown in Fig. 7, the first peak after 20 min involved a series of biopolymers (Biopolymers) with organic colloids and proteins consisting of more than 20,000 g mol^{-1} of MW. The second and third peaks represented humic substances (Humics) and building blocks (polycarboxylic acid) (Building blocks), which showed a MW range from approximately 1,000 to 350–500 g mol^{-1}, respectively. The fourth peak had organic acids of low MW (LMW acids) as its main component. The fifth peak also contained low MW of neutral substances (LMW neutrals) and amphiphilic species (amino

Table 3
Spectral characteristics of the three components identified by parallel factor analysis in this study, and comparisons with other studies. The values in parentheses denote the second maxima of the component

Component	Ex/Em	Description	Reference
Component 1	250(325)/400	Microbial humic-like fluorescence and humic and fulvic substances	C4: (250)325/416 [31] C6: <250(320)/400 [32] G2: 250(320)/400 [33]
Component 2	250(350)/450	Terrestrial humic-like fluorescence in high nutrient and wastewater-influenced environments	C1: <250(370)/464 [34] C4: 250(340)/438 [35] C4: 250(360)/440 [36] C8: <260(355)/434 [36] C2: (250,340)/430 [34]
Component 3	280/330	Tryptophan-like substances (protein-like)	C4: 275/306 [37] C7: 280/344 [36] C8: 275/360 [37] C6: 250(290)/356 [38] Peak B: 275/310 [39]
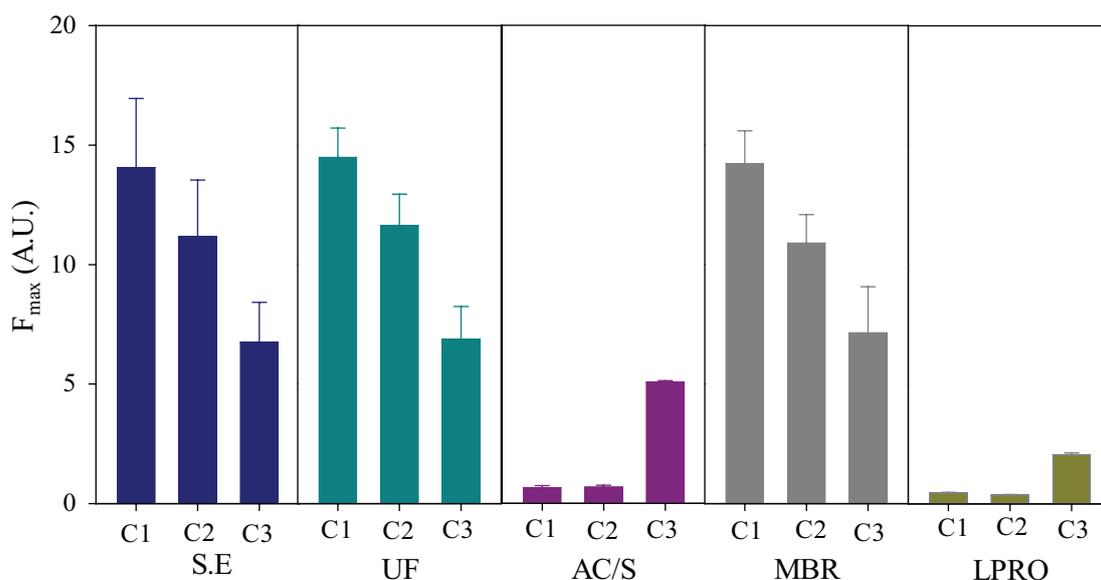
Fig. 6. Maximum fluorescence intensities (F_{max}) after parallel factor analysis component of sewage effluent (S.E) without pretreatment, ultrafiltration (UF), activated carbon/sand filter (AC/S), membrane bioreactor (MBR), and low-pressure reverse osmosis (LPRO)-treated waters.

acid, alcohol, aldehyde, and ketone, among others) with MWs of less than 350 g mol⁻¹ as the main components. In this study, all samples had a DOC concentration of approximately 2 mg L⁻¹ or less, and the percentage of DOC of each peak was calculated by integrating the areas of each peak. Table 4 presents the DOC percentages of each substance in the samples.

The LC-OCD chromatogram of the sewage effluent showed that neutrals constituted the highest portion of total DOC at 34.4%, followed by 28.4% for humic substances, 27.9% for building blocks, and 9.3% for biopolymers (also shown in Fig. 8). As for the UF and MBR-treated samples, the overall proportions of each fraction were similar to those of the sewage effluent, along with decreases in biopolymers (5.1% and 6.7% for the UF and AC/S-treated samples, respectively) and slight increases in neutral substances (41.1% and 42.2% for the UF and AC/S-treated samples, respectively). These results implied that DOC removal by UF or MBR pretreatment of sewage effluent occurred mostly in biopolymers, which may not respond well to fluorescence detection, which was why the PARAFAC results presented almost the same trends in F_{max} values for the three components. Meanwhile, AC/S or LPRO-treated water showed considerable changes in the fractional shares of each constituent, which also agreed with the results of PARAFAC modeling, and neutral

components accounted for the greatest proportion in both samples (96.4% and 98.7% in the AC/S and LPRO-treated samples, respectively). The combination with the PARAFAC components meant that C3 may have been closely related to the low molecular weight (LMW) and neutral components of organic matter.

3.6. Correlations

To better understand the properties of the components identified by PARAFAC, the relationships between each component and the SUVA values of all pretreated samples were observed. SUVA, which is defined as UV absorbance (usually at 254 nm) times 100 divided by DOC, is indicative of the hydrophobicity or aromaticity of natural organic matter; thus, the higher value, the more hydrophobic or aromatic the organic matter. As seen in Fig. 9, C1 and C2 presented moderately strong linear relationships with SUVA, with R^2 values of 0.63 (C1) and 0.61 (C2) at $p < 0.01$. However, C3 showed a negative correlation with SUVA, thereby indicating that C3 contained hydrophilic organics with fluorescence, such as protein-like substances. The relationships presented in this study ascertain that PARAFAC and UV absorbance can be a good tool for the analyzing the structure of natural organic matter [41].
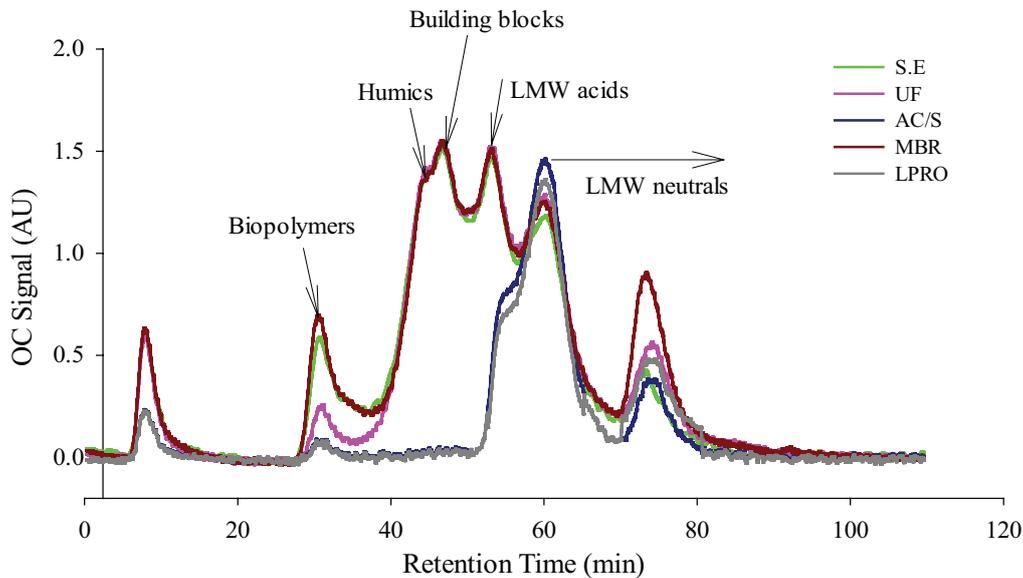
Fig. 7. LC-OCD chromatograms of sewage effluent (S.E) without pretreatment, ultrafiltration (UF), activated carbon/sand filter (AC/S), membrane bioreactor (MBR), and low-pressure reverse osmosis (LPRO)-treated waters.

Table 4
Percentage (%) and dissolved organic carbon (DOC) (mg L⁻¹) of each constituent of the samples. The values in parentheses denote DOC

Fractions	Sewage effluent (S.E) without pretreatment	UF	AC/S	MBR	LPRO
Humic substances	28.4 (0.61)	24.8 (0.53)	–	24.9 (0.58)	–
Building blocks	27.9 (0.60)	29.0 (0.620)	1.4 (0.013)	26.2 (0.610)	–
LMW acids	–	–	0.8 (0.007)	–	0.8 (0.002)
LMW neutrals	34.4 (0.74)	41.1 (0.89)	96.4 (0.89)	42.2 (0.99)	98.7 (0.35)
Biopolymers	9.3 (0.199)	5.1 (0.110)	1.4 (0.013)	6.7 (0.160)	0.5 (0.002)
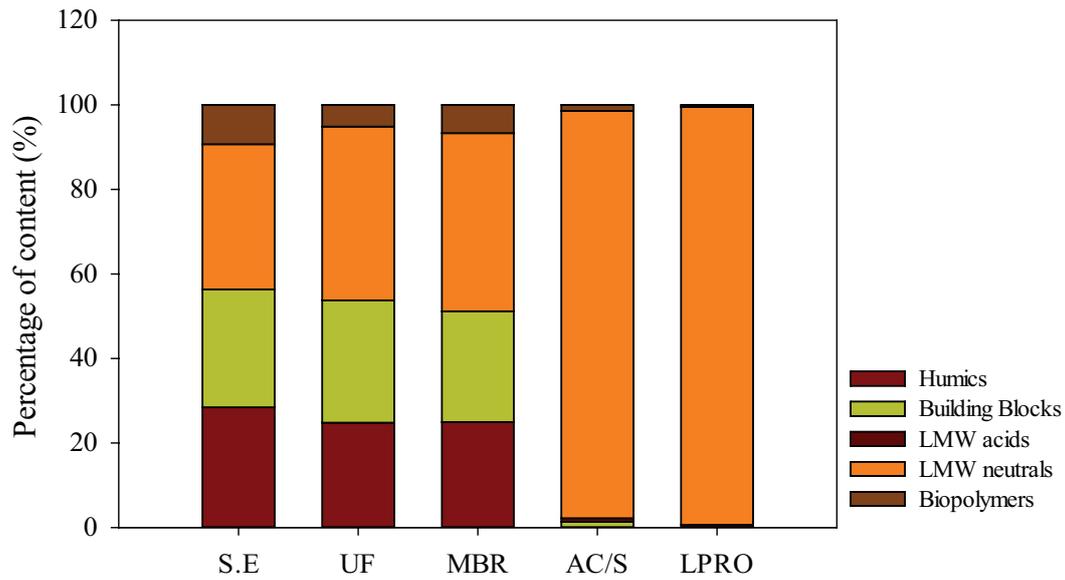
Fig. 8. Fractions of constituents according to liquid chromatography-organic carbon detector chromatograms of the sewage effluent (S.E) without pretreatment, ultrafiltration (UF), membrane bioreactor (MBR), activated carbon/sand filter (AC/S), and low-pressure reverse osmosis (LPRO)-treated waters.

(a)

(b)

(c)
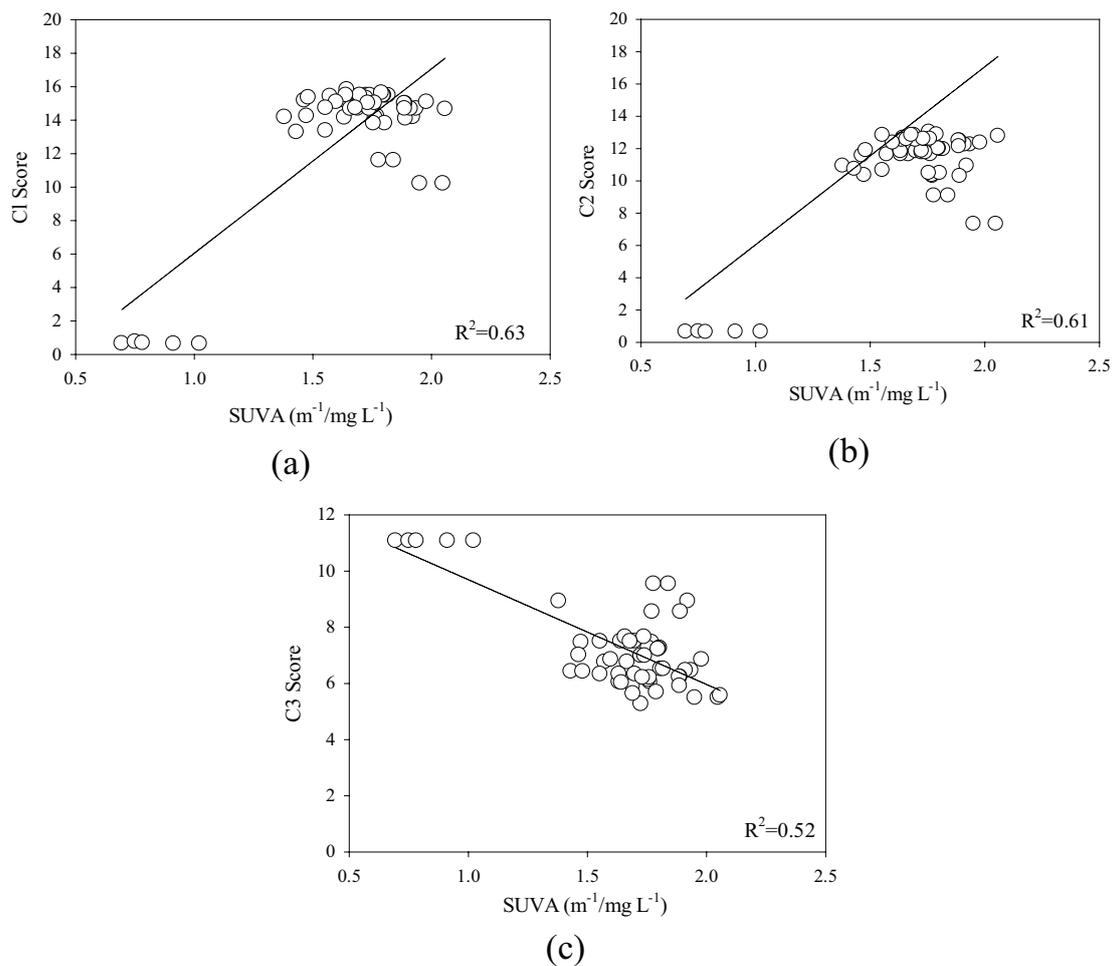
Fig. 9. Correlations between the SUVA and maximum fluorescence intensities (F_{max}) values of the parallel factor analysis components; (a) component 1, (b) component 2, and (c) component 3.

4. Conclusions

The following conclusions were reached through this study, which was based on the results of analyzes of organic matter that affected membrane fouling of the PRO process found by conducting F-EEMs, PARAFAC, and LC-OCD analyzes of pretreated PRO water samples.

- There were strong correlations between the PRO power densities and organic matter in the feed solution.
- The results of the F-EEMs analysis, which analyzed the properties of the organic matter in the wastewater effluent, indicated the existence of a tryptophan-like (protein-like) peak, which is a characteristic property of aromatic proteins, and the existence of a fulvic and humic peak.
- Given that flux reduction was found less in the PRO measurement results of the AC/S-treated water than in those of the UF-treated water, a process that removes fulvic and humic peaks, which are factors that produce fouling in the PRO process, needs to be prioritized. Also, for processes that can reduce foulants more effectively than AC/S processes, pretreatment technologies that can affect biodegradable low molecular structure substances with protein-like (tryptophan) peaks need to be considered.
- Using the database acquired from F-EEMs measurements to perform PARAFAC modeling, three major peaks indicating humic and fulvic components, terrestrial humic-like components, and protein-like (tryptophan) components were identified. Using these findings, major changes in the peaks of the PRO pretreatment processes could be analyzed.
- The LC-OCD analysis results indicated that the main foulants of the PRO membrane were humic substances, building blocks, neutral substances, and biopolymers.
- The F-EEMs-PARAFAC modeling and LC-OCD analysis methods can be used to determine a useful tool to monitor the effect of organic matter foulants on the PRO membrane.

References

[1] N. Ghaffour, T.M. Missimer, G.L. Amy, Technical review and evaluation of the economics of water desalination: current and future challenges for better water supply sustainability, Desalination, 309 (2013) 197–207.
[2] T.Y. Cath, A.E. Childress, M. Elimelech, Forward osmosis: principles, applications, and recent developments, J. Membr. Sci., 281 (2006) 70–87.
[3] S. Loeb, Large-scale power production by pressure-retarded osmosis, using river water and seawater passing through spiral modules, Desalination, 143 (2002) 115–122.
[4] S. Loeb, Production of energy from concentrated brines by pressure retarded osmosis I. Preliminary technical and economic correlations, J. Membr. Sci., 1 (1976) 49–63.
[5] K. Saito, M. Irie, S. Zaitsu, H. Sakai, H. Hayashi, A. Tanioka, Power generation with salinity gradient by pressure retarded osmosis using concentrated brine from SWRO system and treated sewage as pure water, Desal. Wat. Treat., 41 (2012) 114–121.
[6] M. Kurihara, M. Hanakawa, Mega-ton Water System: Japanese national research and development project on seawater desalination and wastewater reclamation, Desalination, 308 (2012) 131–137.
[7] A. Tanioka, Preface to the special issue on "Pressure Retarded Osmosis in Megaton Water System Project," Desalination, 389 (2016) 15–17.
[8] H. Sakai, 2015, Energy Recovery by PRO Systems JDA/Megaton Project/PRO System, IDA Conference, APDA & JDA Joint Forum.
[9] J. Chen, B. Gu, E.J. LeBoeuf, H. Pan, S. Dai, Spectroscopic characterization of the structural and functional properties of natural organic matter fractions, Chemosphere, 48 (2002) 59–68.
[10] J. Chen, E.J. LeBoeuf, S. Dai, B. Gu, Fluorescence spectroscopic studies of natural organic matter fractions, Chemosphere, 50 (2003) 639–647.
[11] L. Fan, T. Nguyen, F.A. Roddick, J.L. Hariis, Low-pressure membrane filtration of secondary effluent in water reuse: pre-treatment for fouling reduction, J. Membr. Sci., 320 (2008) 135–142.
[12] T. Persson, M. Wedborg, Multivariate evaluation of the fluorescence of aquatic organic matter, Anal. Chim. Acta., 434 (2001) 179–192.
[13] S.K. Ishii, T.H. Boyer, Behavior of reoccurring PARAFAC components in fluorescent dissolved organic matter in natural and engineered systems: a critical review, Environ. Sci. Technol., 46 (2012) 2006–2017.
[14] C.A. Stedman, S. Markager, R. Bro, Tracing dissolved organic matter in aquatic environments using a new approach to fluorescence spectroscopy, Mar. Chem., 82 (2003) 239–254.
[15] S.S. Kavurmaci, N.C. Birben, A. Tomruk, M. Bekbolet, Characterization of organic matter in natural waters by EEM fluorescence properties, Desal. Wat. Treat., 57 (2016) 2428–2436.
[16] R.H. Peris, C. Halle, H. Budman, C. Moresoli, S. Peldszus, P.M. Huck, R.L. Legge, Identifying fouling events in a membrane-based drinking water treatment process using principal component analysis of fluorescence excitation-emission matrices, Water Res., 44 (2010) 185–194.
[17] H. Yu, F. Qu, H. Chang, S. Chao, X.L.G. Aou, H. Liang, Understanding ultrafiltration membrane fouling by soluble microbial product and effluent organic matter using fluorescence excitation-emission matrix coupled with parallel factor analysis, Int. Biodeterior. Biodegrad., 102 (2015) 56–63.
[18] M. Bieroza, A. Baker, J. Bridgeman, Relating freshwater organic matter fluorescence to organic carbon removal efficiency in drinking water treatment, Sci. Total Environ., 407 (2009) 1765–1774.
[19] S. Baghoth, S. Sharma, G. Amy, Tracking natural organic matter (NOM) in a drinking water treatment plant using fluorescence excitation-emission matrices and PARAFAC, Water Res., 45 (2011) 797–809.
[20] R.K. Henderson, N. Subhi, A. Antony, S.J. Khan, K.R. Murphy, G.L. Leslie, V. Chen, R.M. Stuetz, P. Le-Clech, Evaluation of effluent organic matter fouling in ultrafiltration treatment using advanced organic characterization techniques, J. Membr. Sci., 328 (2011) 50–59.
[21] J.-Y. Tian, M. Ernst, F. Cui, M. Jekel, Correlation of relevant membrane foulants with UF membrane fouling in different waters, Water Res., 47 (2013) 1218–1228.
[22] S.A. Baghoth, S.K. Sharma, G.L. Amy, Tracking natural organic matter (NOM) in a drinking water treatment plant using fluorescence excitation-emission matrices and PARAFAC, Water Res., 45 (2011) 797–809.
[23] K.R. Murphy, K.D. Butler, R.G.M. Spencer, C.A. Stedmon, J.R. Boehme, G.R. Aiken, Measurement of dissolved organic matter fluorescence in aquatic environments: an inter-laboratory comparison, Environ. Sci. Technol., 44 (2010) 9405–9412.
[24] T. Larsson, M.D. Wedborg, D. Turner, Correction of inner-filter effect in fluorescence excitation-emission matrix spectrometry using Raman scatter, Anal. Chim. Acta., 583 (2007) 357–363.

[25] A.J. Lawaetz, C.A. Stedmon, Fluorescence intensity calibration using the Raman scatter peak of water, Appl. Spectrosc., 63 (2009) 936–940.

[26] C.A. Stedmon, R. Bro, Characterizing dissolved organic matter fluorescence with parallel factor analysis: a tutorial, Limnol. Oceanogr. Methods., 6 (2008) 572–579.

[27] R. Bro, PARAFAC, Tutorial and applications, Chemom. Intell. Lab. Syst., 38 (1997) 149–171.

[28] H. Yu, F. Qu, H. Liang, Z.S. Han, J. Ma, S. Shao, H. Chang, G. Li, Understanding ultrafiltration membrane fouling by extracellular organic matter of *Microcystis aeruginosa* using fluorescence excitation-emission matrix coupled with parallel factor analysis, Desalination, 337 (2014) 67–75.

[29] A. Achilli, T.Y. Cath, A.E. Childress, M. Elimelech, Power generation with pressure retarded osmosis: an experimental and theoretical investigation, J. Membr. Sci., 343 (2009) 42–52.

[30] J.A. Leenheer, J.P. Croue, Characterizing aquatic dissolved organic matter, Environ. Sci. Technol., 37 (2003) 18A–26A.

[31] C.A. Stedmon, S. Markager, Resolving the variability in dissolved organic matter fluorescence in a temperate estuary and its catchment using PARAFAC analysis, Limnol. Oceanogr., 50 (2005) 686–697.

[32] K.R. Murphy, A. Hambly, S. Singh, R.K. Henderson, A. Baker, R. Stuetz, S.J. Khan, Organic matter fluorescence in municipal water recycling schemes: toward a unified PARAFAC model, Environ. Sci. Technol., 45 (2011) 2909–2916.

[33] H. Xu, H. Cai, G. Yu, H. Jiang, Insights into extracellular polymeric substances of cyanobacterium *Microcystis aeruginosa* using fractionation procedure and parallel factor analysis, Water Res., 47 (2013) 2005–2014.

[34] C.A. Stedmon, S. Markager, Tracing the production and degradation of autochthonous fractions of dissolved organic matter using fluorescence analysis, Limnol. Oceanogr., 50 (2005) 1415–1426.

[35] K.R. Murphy, C.A. Stedmon, T.D. Waite, G.M. Ruiz, Distinguishing between terrestrial and autochthonous organic matter sources in marine environments using fluorescence spectroscopy, Mar. Chem., 108 (2008) 40–58.

[36] G.H. Yu, P.J. He, L.M. Shao, Novel insights into sludge dewaterability by fluorescence excitation-emission matrix combined with parallel factor analysis, Water Res., 44 (2010) 797–806.

[37] R.M. Cory, D.M. McKnight, Fluorescence spectroscopy reveals ubiquitous presence of oxidized and reduced quinones in dissolved organic matter, Environ. Sci. Technol., 39 (2005) 8142–8149.

[38] P.G. Coble, Characterization of marine and terrestrial DOM in seawater using excitation emission matrix spectroscopy, Mar. Chem., 51 (1996) 325–346.

[39] S.A. Baghoth, M. Dignum, A. Grefte, J. Kroesbergen, G.L. Amy, Characterization of NOM in a drinking water treatment process train with no disinfectant residual, Water Sci. Technol. Water Supply, 9 (2009) 379–386.

[40] P. Kowalczuk, W.J. Cooper, M.J. Durako, A.E. Kahn, M. Gonsior, H. Young, Characterization of dissolved organic matter fluorescence in the South Atlantic Bight with use of PARAFAC model: relationships between fluorescence and its components, absorption coefficients and organic carbon concentrations, Mar. Chem., 118 (2010) 22–36.

[41] R.A. Al-Juboori, T. Yusaf, P.A. Pittaway, Exploring the correlations between common UV measurements and chemical fractionation for natural waters, Desal. Wat. Treat., 57 (2016) 16324–16335.